BNL-104626-2014-TECH

AGS/AD/Tech Note No. 199;BNL-104626-2014-IR

SPILL STRUCTURE IN THE AGS 10 Hz - 1000 Hz

L. Ahrens

April 1984

Collider Accelerator Department

Brookhaven National Laboratory

U.S. Department of Energy

USDOE Office of Science (SC)

DISCLAIMER

Accelerator Department
BROOKHAVEN NATIONAL LABORATORY
Associated Universities, Inc.
Upton, New York 11973

AGS Division Technical Note
No. 199

SPILL STRUCTURE IN THE AGS 10 Hz - 1000 Hz

L. Ahrens, J.W. Glenn, J. Keane, R. Sanders
April 24, 1984

Summary:

AGS spill structure at frequencies less than 1 KHz is measured using the Fourier analysis of digitized signals from available monitors. A search is made for the source of the observed structure among likely candidates (magnet power supplies) both by noting synchronization between the structure and possible sources; and by measuring both the sensitivity of the spill to ripple on particular magnet strings, and the magnet ripple actually present on those strings.

Introduction:

This paper reports a number of findings from studies carried out parasitically near the close of FY83 SEB running.

As an introduction the topics to be covered will be briefly mentioned. Measurements of spill structure obviously require a spill monitor. A brief discussion of monitors used is included. One possible contamination on these signals is noise at power frequencies (n x 60 Hz). For one subset of the measurements to be described (spill sensitivity) such noise irrelevant. For the spill measure itself noise at the frequencies of interest contaminates the signal and must be estimated. This is attempted by comparing independent monitors.

The measuring apparatus which accepts either this spill signal or any other driving signal involves signal filtering, attenuation, digitization with appropriate synchronization, Fourier analysis, and result presentation. The system will be described.

Using signal and system, two studies are carried out. The first involves driving a particular magnet string power supply with a selected frequency component (measured using the system) and observing any resulting spill structure at that frequency. Because the frequencies employed are chosen to be near but not at power frequencies (e.g., not multiples of 60 Hz), power frequency pick-up on the signals to be measured is irrelevant. The second study uses the ability of the system to (by proper synchronization) enhance a given spill component relative to others. In particular structure synchronized to "LILCO" (the AC line power) can be enhanced or suppressed relative to structure synchronized to "Siemens" (the Main Magnet power supply fundamental rotation frequency). Here spill monitor noise affects the results.

We will discuss the measuring system, the spill signals themselves and then turn to the data. Calibration is discussed in an appendix.

Measuring System:

This system (see Fig. 1) starts with an analogue signal at the injection console in the Main Control Room and ends with a discrete Fourier spectrum of that signal with the option of enhancement depending on synchronization to an external signal. The analogue signal is typically filtered to contain frequencies between 20 hz and 1 Khz (3 dB points) using an active high input impedance filter). The low frequency cut removes a DC offset which would reduce the dynamic range available from the digitizer; the high frequency cut suppresses "aliasing" in the calculated Fourier transform should higher frequency components be present. The output is passively attenuated to contain voltage excursions less than .5 volts to avoid saturating the digitizer which follows. Both the

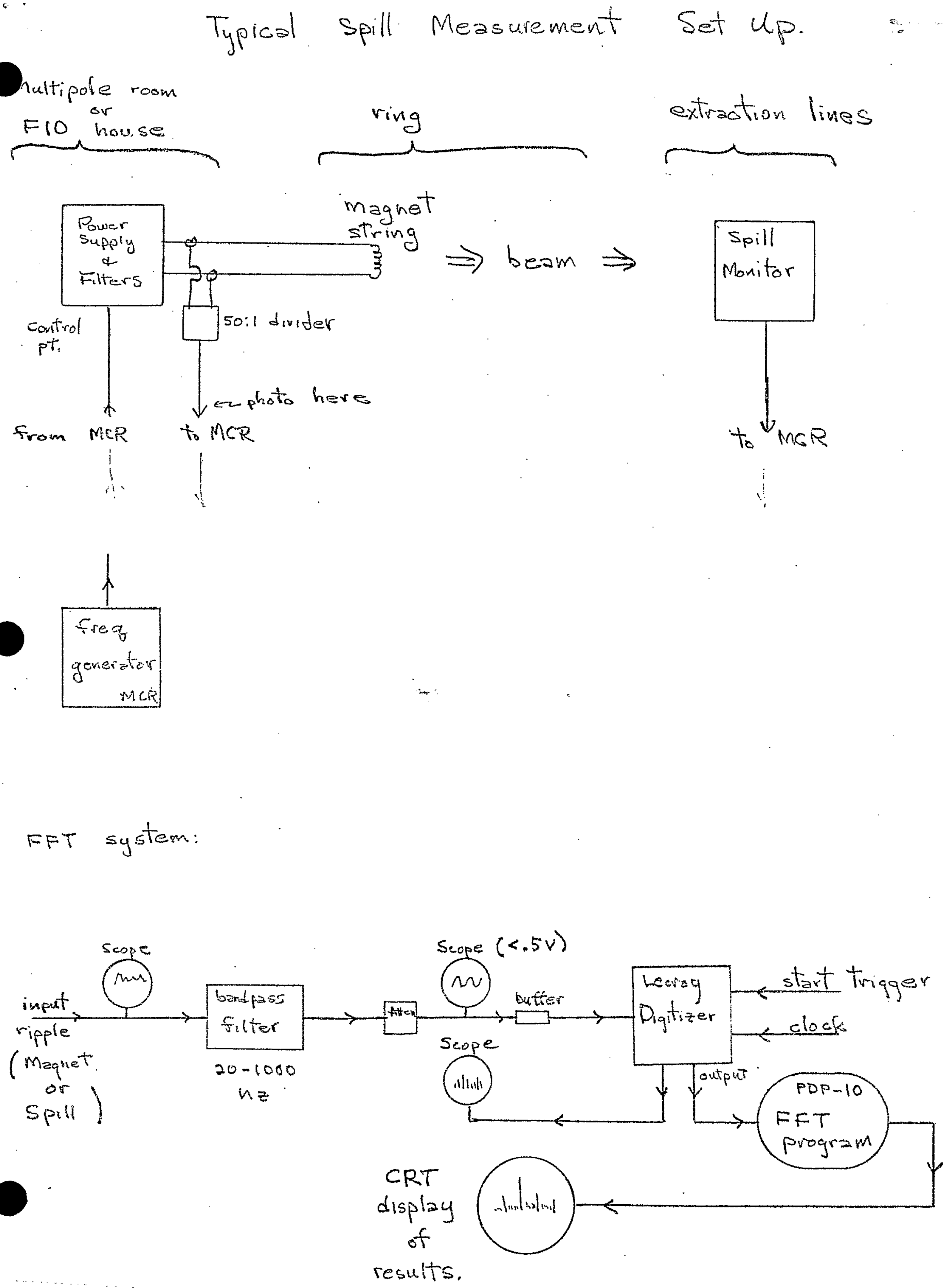
Typical Spill Measurement Set Up.
multipole room or F10 house
ring
extraction lines
Power Supply & Filters
magnet string
beam
Spill Monitor
50:1 divider
control pt.
photo here
from MCR
to MCR
to MCR
freq generator MCR
FFT system:
Scope
input ripple (Magnet or Spill)
bandpass filter
20-1000 Hz
Atten
Scope (<.5V)
buffer
Scope
Lecroy Digitizer
start trigger
clock
output
PDP-10 FFT program
CRT display of results.

Fig. 1

starting time and the digitization frequency of the digitizer are controlled from the injection console. The digitization rate is set to either a 1.024 KHz or 2.048 KHz clock. The start of digitization can be synchronized to an external signal--for example the crossing of zero with positive slope of a LILCO signal--to the precision of the internal 1 MHz crystal frequency of the clock generator. The reason for these particular digitizing frequencies is a result of the capacity of the digitizer (1024 slots) and the properties of the discrete Fourier transform which is to be applied to the stored data. In particular, the finite length of the digitization sampling period, (the "window"), results in a sample with abrupt boundaries at the start and stop times. The Fourier components which the program calculates are those which would result if the late boundary were superimposed on the early boundary and the pattern continued forever. One result from this is that any frequency which is contained within the "window" an integer number of times is handled "perfectly" while for example one contained for $n + \frac{1}{2}$ wave lengths will have large discontinuities at the edges. The transform in the latter case will contain what appear to be spurious frequency components, and in particular will show a spread over a band of frequencies. By choosing the sampling frequency such that the window is exactly 1 second long (1.024 KHz) all integer frequencies are properly treated. In this case the integration time (1 sec) includes the bulk of the spill (spill length ~ 1.5 sec typically) and frequencies up to 500 Hz are measurable. Choosing a digitizing frequency of 2.048 KHz gives information up to 1 kHz, properly treats only even frequencies, and samples only 500 ms of spill. Since there is an interest in structure at 720 Hz this mode is frequently employed.

The synchronization of the start of the window either to LILCO (60 Hz) or the Siemen shaft frequency allows a separation of spill structure causes. The data analysis software allows a mode where the information from successive digitizations is simply averaged before any transformation is carried out. In this way any component which is moving randomly in phase relative to the synchronizing signal will be suppressed proportional to the square root of the number of iterations included in the average.

Another option allowed by the analysis package is the averaging of the Fourier components from any number of iterations which gives the average character of the data, the net problem to be suppressed.

Spill Signals:

The reference spill signal in most of the data taking uses a secondary emission monitor identified as "CE10". All of the extracted beam passes through the detector, which consists of a series of thin plates. The current from one plate is amplified, transmitted to the MCR vicinity, and multiplexed to the injection console. The resulting signal is proportional to the flux through the detector with a frequency response extending beyond the region explored, though not necessarily flat.

In addition to this detector, there are many others which provide what should be redundant or near--redundant information. Those investigated include scintillator telescopes viewing the A, B, or C target, and air ionization chambers (STAKSs) in the A, B, and C lines. The "noise" in the Fourier transformers clearly show than the telescope signals attenuate less rapidly with frequency that CE10 (~ x2 at 720 Hz if equal at 150 Hz) while the STAK signals fall more rapidly with frequency (~ 1/2 at 720 Hz, if equal at 150 Hz). The Fourier transforms of five extractions were averaged from each detector for unchanged machine conditions. The resulting peaks at multiples of 60 Hz, when above noise, normalized to the smooth noise signal at ~150 Hz are tabulated in Table I. The relative frequency responses are not corrected out. The two lines for BTEL are taken at two intensities in the B line. For CE10, a 10% spill modulation (pk-pk) corresponds to 3.2 counts. (See Appendix 2.) For comparison, the responses from the other counters are normalized to be equal to CE10 at 150 Hz.

TABLE I

Spill Signals Normalized to CE10 Using Observed <Signal> @ 150 Hz

Source Frequency:	60	120	180	300	360	420	720	<Signal> in counts @ 150 Hz
CE10 (Implied spill modulation)	12 (38%)	3 (9%)	0	0	19 (60%)	0	3 (9%)	2
ATEL	10	0	7	4	26	0	8	.6
BTEL 1	18	0	9	3	15	0	7	.4
BTEL 2	15	0	6	0	7	0	2	.55
CTEL	10	0	3	4	14	0	4	1.4
ASTAK	38	5	4	3	11	0	4	2
BSTAK	22	6	0	0	16	2	2	2.2
CSTAK	14	0	0	2	10	0	1	4

The table shows the motivation for this study. All the monitors agree that the spill has large structure at 60 Hz and 360 Hz.

The variation between monitors, as well as with time on a given monitor is fairly large, but an underlying structure is clear. Most of what follows will use CE10 as a spill monitor.

Siemens Sync. vs LILCO Sync.:

The CE10 frequency spectrum can be measured so as to isolate either LILCO synchronized or Siemens synchronized components. In the former case the digitization begins "in time" with a positive slope zero crossing of a "60 cycle" signal coming directly from the power line. The Siemen synchronization is similarly taken relative to a signal derived from the Siemens' shaft phase frequency. The measured relative phases of these signals are seen to be nearly uncorrelated. As a check on this a pure LILCO signal is analyzed with the Siemens synch timing. A single shot reports an amplitude at 60 Hz of A_1 = 117; an average over 50 shots reports a 60 Hz amplitude of A_{50} = 18.5, whereas the "random walk" model predicts $A_{50} = A_1/\sqrt{N} = A_1/7 = 16.7$. Table II gives the results of 50 extractions analyzed synced the two ways. The errors shown are estimates resulting from repeating the experiment. The "derived" rows correct for the cross talk. Single shot rows give unaveraged data taken at the same time. One unanticipated conclusion is that this monitor sees large components, dominant at 60 Hz but significant at 360 which are not LILCO synced but rather remain in step with the Siemens' set.

TABLE II: Spill Modulation vs Synchronization

Sync	(Hz) Freq: 60	120	180	240	300	360	720
Single Shot	11	5	2	3	2.6	15	6
Single Shot	7.7	3	1	2	2	10	---
LILCO	4.3±.1	2.8±.3	1.4±.1	1.5±.3	1.1±.1	14.7±2	4.1
Siemen	8.8±.3	2.0±.4	.25±.1	1.1±.1	.6	4.0±.4	2
Derived LILCO	4.1±1	2.8±.3	1.4±.1	1.5±.3	1.1±.1	14.7±2	4.1
Implied Spill Modulation	(13±.3)%	(9±1)%	(4±.3)%	(5±1)%	(3±.3)%	(46±6)%	18%
Derived Siemen	8.8±.3	2.0±.4	.15±.17	1.1±.1	.6	3.4±.5	2
Implied Spill Modulation	(28±1)%	(6±1)%	(.5±.5)%	(3±.3)%	(2±)%	(11±2)%	6%

Magnet String Ripple vs Spill Ripple:

The central effort to the study was the measurement of the effectiveness of ripple on each of the various magnet strings in exciting spill structure at that frequency. This was measured at a series of frequencies over the range under discussion, which information when combined with measurement of the actual voltage ripple present on the magnet strings, allows a prediction of the spill ripple due to the string. In all cases an electrical reference point in the power supply allowed introduction of ripple at an arbitrary frequency. The voltage on the output of the supply, after any filters, was then sampled and sent back to the MCR for Fourier analysis. Indeed the sample point relative to filter attenuation etc., is critical only in that the same point be used when the "natural" magnet ripple is measured. The frequencies used spanned the range of interest (60 - 360 Hz) but avoided multiples of 60 Hz. While driving the magnet at a measured amplitude, the amount of spill ripple was measured at that frequency, again using CE10 and the Fourier analysis program. The resulting ratio was observed to be independent of the actual amplitude of the drive provided system saturation was avoided. This procedure was applied to the horizontal and vertical quadrupole strings, the horizontal and drive sextupole strings, the H20 and F10 power back leg windings, the skew sextupole string and, in addition, with some modifications in detail, to the RF cavity main tuning current and to the main ring magnet power supply (Siemens). Figures 2, 3 and 4 give the ratios between driving magnet ripple and resulting spill ripple. The calibration and normalization are discussed in an appendix.

The magnet ripple normally present on each power supply system was measured at the point used for the previous measurements by filtering the output at multiples of 60 Hz, and photographing the resulting wave form. Although the measurements could have been made in the MCR using the Fourier transform system, the above procedure was adopted to minimize any spurious components. The results are given in Appendix 1, Table A3. The bottom line to all of this is Table III.

Inspection of the magnet strings in the table suggests (1) certain of the supplies contribute significantly at 60 Hz and (2) none contribute at 360 Hz.

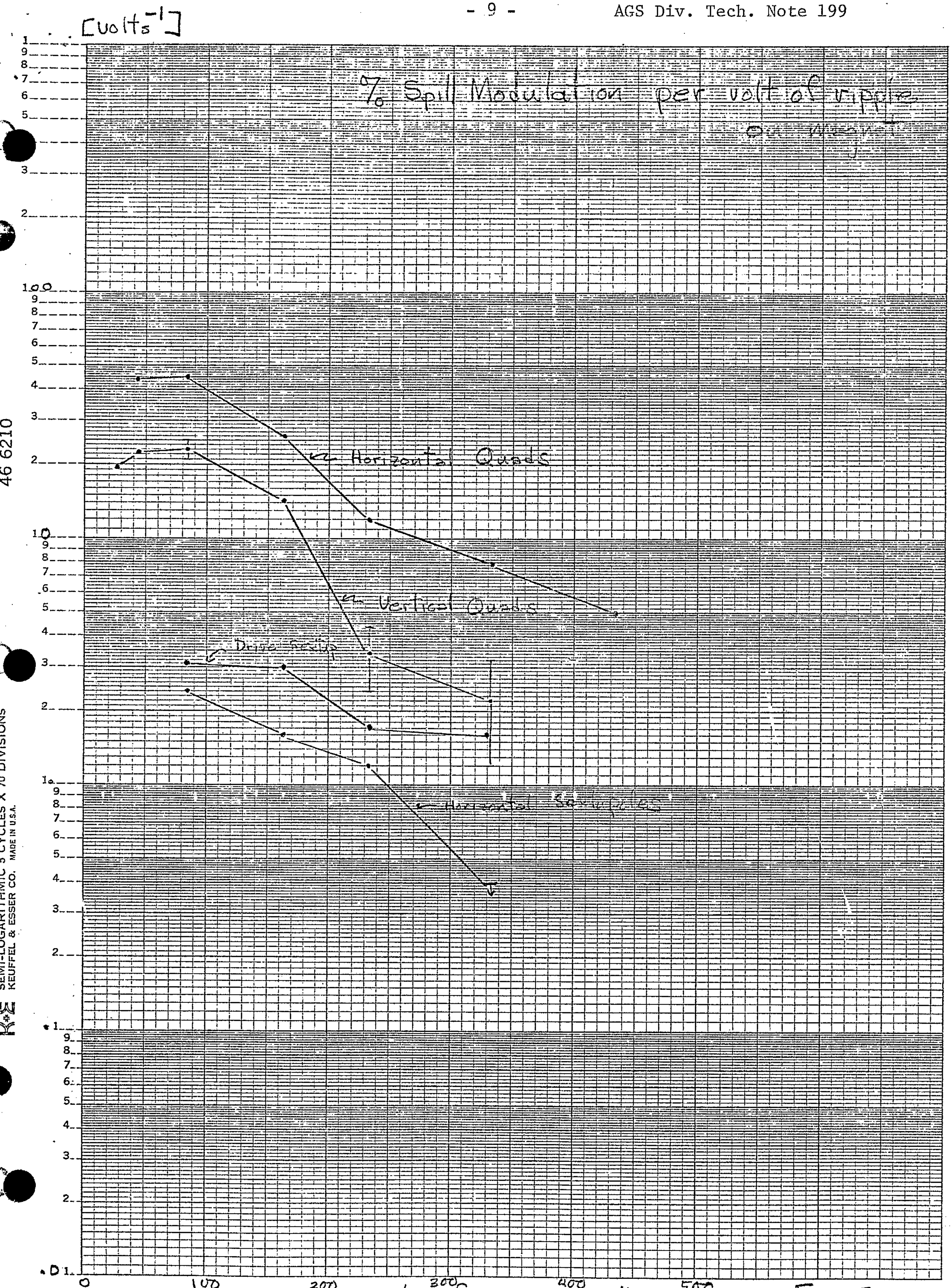
[volts⁻¹]
% Spill Modulation per volt of ripple
← Horizontal Quads
← Vertical Quads
ripple frequency Hz
0
100
200
300
400
500
46 6210
SEMI-LOGARITHMIC 5 CYCLES X 70 DIVISIONS
KEUFFEL & ESSER CO. MADE IN U.S.A.

Fig. 2

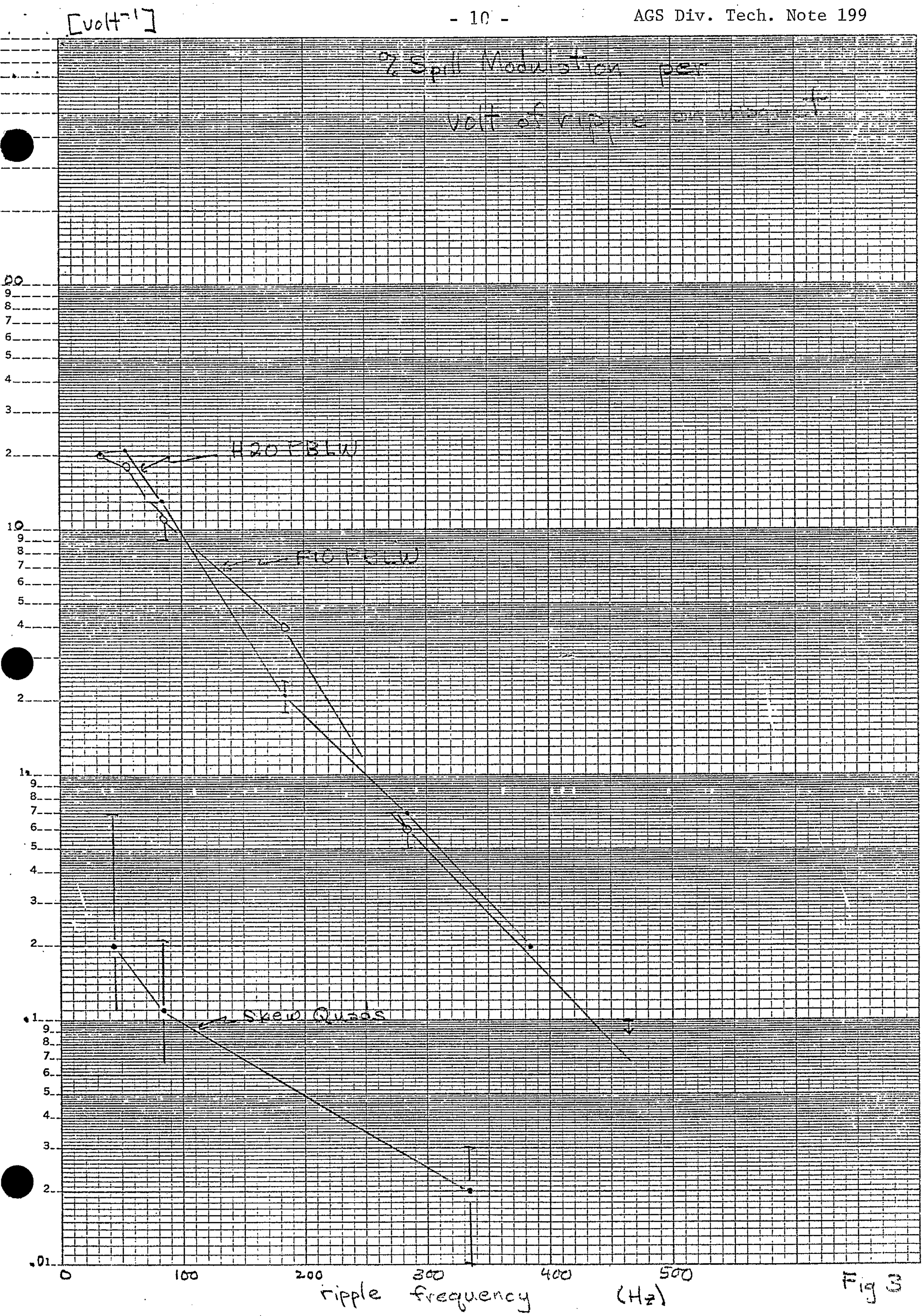
[volt⁻¹]
% Spill Modulation per volt of ripple
H20 CBLW
F10 FCLW
Skew Quads
0
100
200
300
400
500
ripple frequency (Hz)

Fig 3

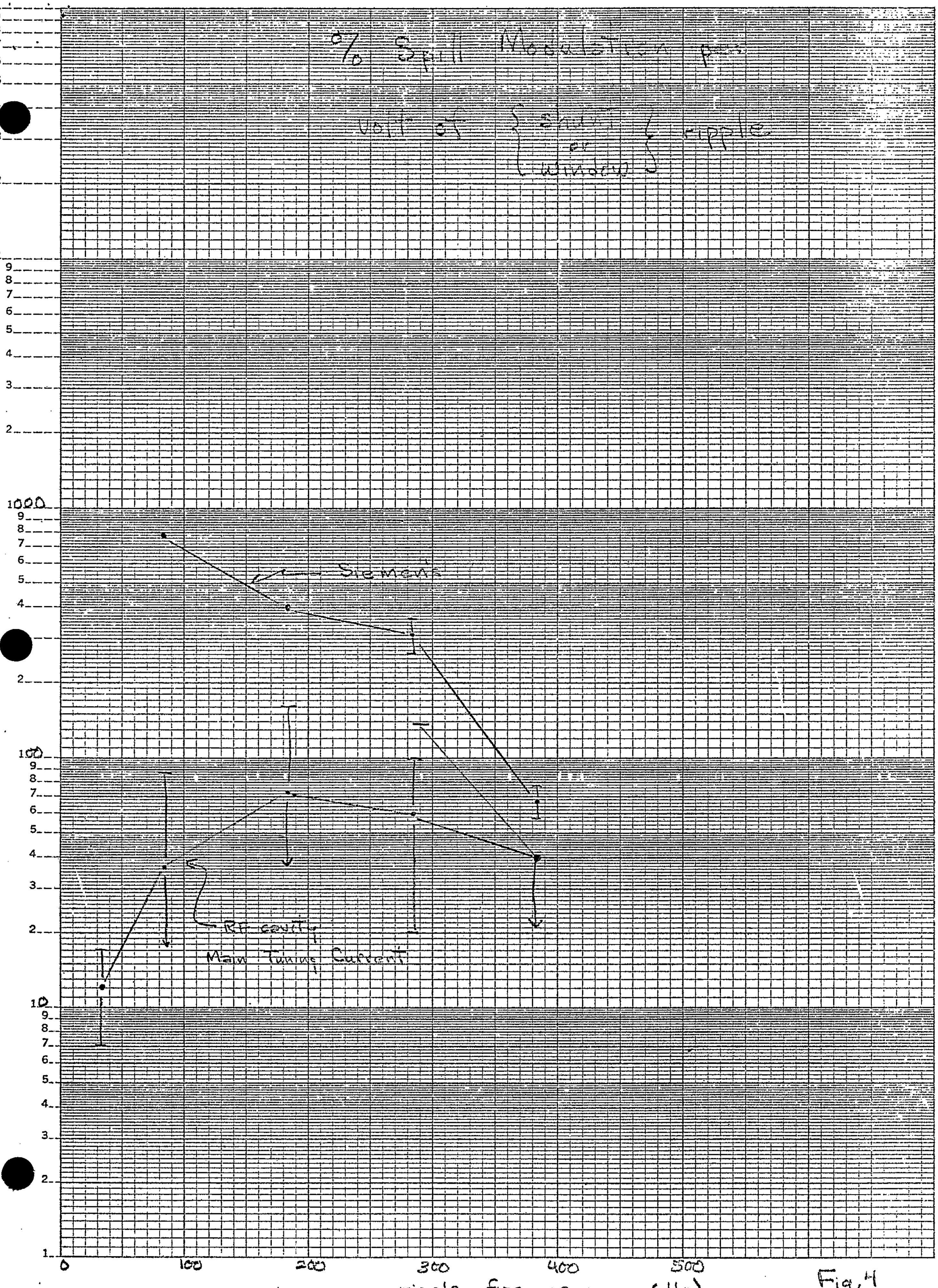
% Spill Modulation per
volt of { shunt or window } ripple
Siemens
RF cavity
Main Tuning Current
1000
100
10
1
0
100
200
300
400
500
ripple frequency (Hz)

Fig. 4

Measurements were not taken of actual magnet ripple on the skew quad string. However, the string runs at 50 volts typically and would need 50 V of ripple to affect the spill by 1% at 360 Hz.

The Siemens study used the two "window" signals as the output monitor points, while ripple was introduced via the "Spill Servo Aux" input. The window signal was not filtered and measured at multiples of 60 Hz so the table numbers are somewhat crude estimates from overall photographs. Here again a significant contribution to spill at 60 Hz is likely, the effect at 360 is small.

The main tuning current in the RF cavities was wiggled with little evidence for resulting spill ripple. The data in Figure 2 primarily reflects poor signal to noise measurements of the spill which presumably would have been improved with higher drive. Natural MTI ripple was not explicitly measured; however, the following qualitative statements can be made. The MTI was driven significantly above its normal ripple with no observed correlated spill ripple.

Finally comparing Table III with Table II, have we any agreement between spill structure observed and spill structure predicted? At 60 Mz we have plenty of potential sources to yield the measured structure, primarily the power back leg windings and Siemens. At 360 Hz, the magnet strings measured seem unable to contribute significantly. The only exception to this is the Siemens, but the 3% ripple expected is small even compared to the 11% Siemens synced component measured. A large 360 Hz component is present on all monitors investigated and its source continues to evade us.

All of these measurements were made at the very end of AGS slow beam running for FY83. There was little repetition of results to check for consistency, and in particular the measurement of ripple present on given magnet strings is very vulnerable to trivial errors. The results need repeating.

Acknowledgements

The FFT software package used in the above was assembled for a different measurement by Dr. J. Claus. Additional software support was provided by John Dabrowski. E. Gill and S. Naase provided technical expertise and support. A. Soukas provided essential ideas.

TABLE III: Predicted Spill Modulation (%)

Magnet Freq: Hz	60	120	180	240	360
Vert Quad	3.5	2.4	.75	.3	.16
Hori Quad	3.8	4.2	.55	.72	.6
Hori Sext	.3	.75	.2	.06	.2
Drive Sext	.3	.9	.4	.8	.5
H20PBLW	15.4	4.2	1.1	.6	.1
F10PBLW	9.	4.	.7	.3	.08
Skew Quad	(10% @ 50V)	see text			(1% @ 50V)
Siemens	60 ± 30				3 ± 1
MTI	see text				

Appendix A: Spill Transfer Function Data

For reference purposes tables of data and reduced data are included herein. Table A1 gives the raw counts returned by the Fourier analysis at the frequency being studied both for the magnet excitation and for the spill. Except as noted, the magnet voltage is attenuated 50:1 at the source. Both magnet signal and spill (CE10 throughout) signal suffer a (.67) attentuation at the filter (20 Hz - 1 kHz 3dB points). Magnet reading with an "a" subscript were further reduced by the factor (.37), "b" were reduced by 18dB. Error where shown indicate the spread in repeated measurements and are best estimates for data without explicit errors. The Siemens and r.f. cavity Main Tuning Current (MTI) measurements did not involve the 50:1 attentuation on the effective "magnet" input.

Table A2 uses A1 together with the calibration factors to derive the spill modulation expected for a given amount of voltage ripple on a magnet string. S = spill F.T. counts, M = magnet ripple F.T. counts. The nominal calculation goes as follows:

$$\frac{\%\text{ spill}}{\text{volt on magnet}} = [S \times (3/2) \times (1\%/.32\text{ cnts})] \div$$

$$[M \times (3/2) \times (50) \times (1\text{ Volt}/234\text{ cnts})]$$

or

$$\frac{\%}{\text{Volt}} = \left(\frac{S}{M}\right) \times 14.6$$

where the (3/2) factors are filter attenuation and (50) is magnet attenuation (which for some measurements is further increased as noted). These results are also given in Figures 2 and 3 of the text.

For the Siemens and the MTI we are not measuring magnet voltage, but rather other monitors; and no attenuation is involved. For these the table should be thought of as % spill modulation/volt on the monitor.

To close the loop we need measurements of frequency components on the magnets or monitors during the spill. These are given in Table A3; and finally, the predicted spill contribution in Table III of the text.

Table A1 **M = Magnet** **Raw F.T. Counts**
S = Spill

Frequency (Hz): **Magnet**		**28**	**44**	**84**	**162**	**232**	**332**	**432**
1. Vert. Quad	M	11.1	14.3	9.6	9.5	16	10	
	S	14.8	22	15±1	9.2	3.7±1	1.5±1	
2. Hori. Quad	M		11.3	5.5±1	3.3	3.6	4.4±.1	3±.1
	S		34±1	17	5.9	3±1	2.5±.5	1±.5
3. Hori. Sext	M			42	20.5	12.3± .1	7.3	
	S			7±.5	2.3	1±.5	≤.2	
4. Drive Sext	M			22.4	13.2±.1	10.3±.1	9.4	
	S			4.8±.1	2.7±.1	1.2	1±.5	
(freq.)		34	54	(84)	184	284	384	
5. H2OPBLW	M	8.4±.1	10.7±.1	15.5±.1	35±5	(9.35±.1)[a]	(7.9±.1)[a]	
	S	12.1±.3	16±1	13.5±.5	4.5±.5	1.15±.1	.3±.3	
(freq.)				(84)	134	264	464	
6. F1OPBLW	M	2.1	(2.6)[a]	(4.1)[a]	(6±.05)[a]	(13)[a]	(28)[a]	
	S	7.6±. 2	8.8± .1	7.5±.1	4±1	1.4±.2	.5±.5	
(freq.)			44	(84)		(334)		
7. SKEW Quad	M		10.5)[b]	(14.1)[b]		(24±3)[b]		
	S		(1.0±.2	.83± .1		.32±.04		
(freq.)				84	184	284	484	
8. Siemens	W			13.5±.5	6.4±.4	4±.2	8.2±.1	
	S			14.4	3.5	1.7±.3	.75±.1	
(freq.)			(34)				(384)	
9. MTI	I		12.5±.1	8.1±.2	5±.1	3.5±.2	3.9±.1	
	S		.2± .1	.4±.4	.5±.5	.3±.2	.2 ± .6	

TABLE A2

% Spill Modulation/(Volt on Magnet)

frequency (Hz)	28	44	84	162	232	332	432
1. Vert. Quad	19.5	22.5	23±2	14.2	3.4±1	2.2±1	
2. Hori. Quad		44	45	26	12	8	5
3. Hori. Sext			2.4	1.6	1.2	<.4	
4. Drive Sext			3.1	3.0	1.7	1.6	
(freq.)	(34)	(54)	(84)	(184)	(284)	(384)	
5. H2OPBLN	21	22	13	2.1±.3	.7	.2	
(freq.)				(134)	(264)		(464)
6. F1OPBLW	20	18	11±2	4	.6±.1		<.1
(freq.)	(44)		(84)			(334)	
7. SKEW Quad	.2±.5		.11±.1			.02±.01	
(freq.)			(84)	(184)	(284)	(384)	
8. Siemen			780	400	310=50	67±10	
(freq.)	(34)		(84)	(184)	(284)	(384)	
9. MTI	12±5		36±40	73±80	60±40	40±100	

Table A3: Measured Power Supple Ripple (volts)(±10%)

Frequency (Hz):	60	120	180	240	360
Vert. Quad.	.15	.125	.075	.1	.08
Hori. Quad.	.085	.12	.025	.06	.09
Hori. Sext.	.1	.375	.125	.05	.55
Drive Sext.	.1	.3	.15	.475	.3
H20PBLW	.7	.6	.5	.5	.3
F10PBLW	.5	.5	.175	.25	.25
SKEW Quad.			?		
Siemens	.05-.1		?		.02-.04
MTI	<< .1		?		<< .03

Appendix 2

Signal Calibration:

The system described above and in Fig. 1 allows for straight forward calibration and checking since a known signal (frequency, voltage) can be fed in and the system response measured. For the standard AC signal the system returns approximately 120 counts for full scale voltage (.5V). To be exact the measured result is 23.4 counts per 100 mV peak to peak input signal, frequency independent. For a D.C. signal 100 mV results in a measured 93.5 count zero frequency response. The D.C. result is just four times the A.C. number (4 x 23.4 = 93.6) as expected from standard Fourier coefficient definitions. This is relevant for transforming spill structure measurements into percentage modulation. In particular for the CE10 monitor the zero frequency component of the spill reported 128 counts under what were nominal conditions for the rest of the measurements: namely a machine intensity of 9×10^{12}, and "effective spill length" of .5, and most directly an integrated spill count on CE10 of 2800-2900 counts. This combined with the previous measure implies that the spill average was 137 mV on the CE10 monitor which agrees with a qualitatively eyeball average using an oscilloscope. Hence for example a ripple on the spill causing a 10% modulation would be 13.7 mV peak to peak or 3.2 A.C. counts. Variations in machine conditions would change this calibration by an order of ±10%, and although the integrated spill count (and beam intensity) were monitored, they generally were not recorded and the effect is not corrected for.

JD
Distribution: A.D. S&P Staff